APPLICATION OF SEMICLASSICAL METHODS TO NUMBER THEORY*

M. Brack

Institute for Theoretical Physics, University of Regensburg
93040 Regensburg, Germany

M.V.N. Murthy

Institute of Mathematical Sciences, Chennai 600 113, India

J. Bartel

Institute Pluridisciplinaire Hubert Curien, CNRS-IN2P3
University of Strasbourg, 67000 Strasbourg, France

(Received February 18, 2020)

We show that semiclassical methods that are traditionally used to describe many-body sytems in physics can also be used to describe partitions that are studied in the number theory within pure mathematics. For the partitions $P(n)$ of a number n into sums of distinct squares, we show that the smooth asymptotic part $P_{\rm as}(n)$ can be well-reproduced by quantum statistical methods, and that its oscillating part $\delta P(n) = P(n) - P_{\rm as}(n)$ is well-reproduced by the periodic orbit theory in terms of a few "orbits" that can be related to Pythagorean triples (m, p, q) of integers with $m^2+p^2 = q^2$.

DOI:10.5506/APhysPolBSupp.13.369

This article is dedicated to the memory of Rajat Bhaduri who left us in November 2019. He had been a decisive partner in much of the work reported here and has actually been the driving force for the development of the study discussed below in more detail. Rajat Bhaduri has been a widely recognized scientist, a marvellous teacher, and a very dear friend.

1. Introduction

Shell effects are an ubiquitous phenomenon in many-fermion systems such as nuclei, atoms, metal clusters or nanostructures. Besides selfconsis-

* Presented at the XXVI Nuclear Physics Workshop *Key problems of nuclear physics*, Kazimierz Dolny, Poland, September 24–29, 2019.

tent microscopic methods such as Hartree–Fock or density functional theory, they have most effectively and most abundantly been described by the shell-correction method invented by Strutinsky [1] half a century ago. Krzysztof Pomorski, whose birthday we are celebrating in this workshop, has also applied this method successfully to nuclei and contributed to its further improvement. Not long after Strutinsky's invention, the semiclassical periodic orbit theory (POT) was developed [2], by which the discrete spectra of quantum systems can be related to the periodic orbits of the corresponding classical systems in terms of the so-called *trace formulae*, both for integrable and for non-integrable and chaotic systems. The POT has also been successfully used to describe gross shell effects in finite quantum systems in terms of the few shortest classical periodic orbits. We refer to the text book [3] for an overview of semiclassical methods and their applications to many different physical systems.

In this contribution, we shall draw attention to the fact that semiclassical methods have also been applied successfully to mathematical objects, namely the so-called *partitions* of a given integer n into various sums involving other integer numbers. For an introduction to this topic, we refer to [4] and to three recent articles involving the present authors [5–7]. In Refs. [4, 5, 7], the focus was on the smooth asymptotic parts $P_{\rm as}(n)$ of various partitions $P(n)$ — which can be obtained by quantum statistical methods that also have semiclassical character — while in [6], the main result was a trace formula reproducing the oscillating part $\delta P(n) = P(n) - P_{\rm as}(n)$ of the number $P(n)$ of ways a given integer n can be written as a sum of distinct squares of integers, in short: of the *distinct square partitions*.

2. Distinct square partitions

In the following, we present a summary of our recent article [6]. We reproduce only the main ideas and some selected results and refer to the full paper for all technical and calculational details.

2.1. Definition and oscillatory behaviour

We define the function $P(n)$ that counts the number of ways in which a given integer n can be written as a sum of distinct squares of positive integers m_i

$$n = \sum_{i=1}^{I_n} m_i^2 \,, \qquad m_i \neq m_j \;\; \text{for} \;\; i \neq j \,. \tag{1}$$

Hereby, the number I_n of summands is not specified. It may start from $I_n = 1$, in which case m_1 is the largest integer $\leq \sqrt{n}$. The highest I_n is limited by $I_n \leq (3n)^{1/3} - 1/2 + \mathcal{O}(n^{-1/3})$. Each particular sum (1) is

called a *partition* of n into squares. The word *distinct* implies that all m_i within each partition must be different. We define $P(0) = 1$ and, trivially, one sees that $P(1) = 1$. The infinite series of numbers given by $P(n)$ for $n = 0, 1, 2, \ldots$ is called the series A033461 in the on-line encyclopedia of integer sequences (OEIS) [8]. Its first ten members are 1, 1, 0, 0, 1, 1, 0, 0, 0, 1 (see also Fig. 2 below).

As was pointed out in Ref. [4], the exact function $P(n)$ for distinct square partitions exhibits pronounced oscillations with a beat-like structure when the points are joined by a continuous curve, as shown in Fig. 1 and Fig. 2 below.

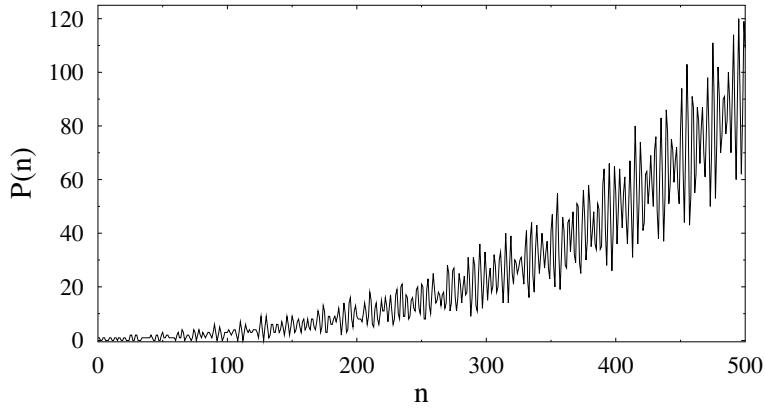

Fig. 1. $P(n)$ of the distinct square partitions shown in the low-n region. Note that $P(n)$ is defined for integer values of n. Here, we have joined the points by a continuous curve to emphasize the beat structure.

Where are these regular oscillations coming from? Consider an integer n that is a sum of squares: $n = m^2 + p^2$. If n itself is a square: $n = q^2$, then the three numbers m, p, q form what is commonly called a Pythagorean triple (PT) of integers (m, p, q) with $m^2 + p^2 = q^2$. Such triples can only occur in square partitions, since Fermat's last theorem [9] asserts that only squares of integers may be written as sums of two (or more) other squares. Since an increasing number of such triples will occur in the counting function $P(n)$ with increasing n, it is quite plausible that they reflect themselves in the oscillatory behaviour of $P(n)$.

For a quantitative analysis, we start from the generating function $Z(\beta)$ which for any given partition $P(n)$ is defined as

$$Z(\beta) = \sum_{n=0}^{\infty} P(n)\, \mathrm{e}^{-n\beta}\,. \tag{2}$$

For the distinct square partitions, it is given by

$$Z(\beta) = \prod_{m=1}^{\infty} \left[1 + \mathrm{e}^{-m^2\beta}\right] = \exp\left\{\sum_{m=1}^{M} \ln\left[1 + \mathrm{e}^{-m^2\beta}\right]\right\}. \tag{3}$$

In principle, M is infinity according to the left-hand side of (3). However, when calculating $P(n)$ with finite n by Eq. (6) below, we have — for the reason given after Eq. (1) — the restriction $M(n) = [\sqrt{n}\,]$, where $[\sqrt{n}\,]$ denotes the largest integer contained in $\sqrt{n}$. The right-hand side of Eq. (3) was also used to generate our data base for the $P(n)$ up to $n = 160\,000$.

In the following, we take β to be a complex variable

$$\beta = x + i\tau\,, \qquad (x, \tau \in \mathrm{R})\,, \tag{4}$$

where x and τ are dimensionless real variables. Note that (3) can be viewed as a fermionic canonical grand partition function with chemical potential $\mu = 0$. Therefore, there is no constraint on the average particle number N which may go up to infinity.

The inverse Laplace transform of $Z(\beta)$ yields the partition density $g(E)$

$$g(E) = \mathcal{L}_E^{-1}[Z(\beta)] = \frac{1}{2\pi i}\int_C Z(\beta)\,\mathrm{e}^{E\beta}\,\mathrm{d}\beta = \sum_{n=0}^{\infty} P(n)\,\delta(E-n)\,, \tag{5}$$

where $\delta(E-n)$ is the Dirac delta function peaked at $E = n$. We denote the dimensionless real argument of $g(E)$ by E because of its relation to the energy in the context of statistical physics, where $g(E)$ is the level density (or density of states) of a system of independent particles. The contour C in (5) runs parallel to the imaginary axis τ with a real part $x = \epsilon > 0$.

In Ref. [6], we have derived the following integral representation for $P(n)$:

$$P(n) = \frac{1}{2\pi}\int_{-\pi}^{\pi} \mathrm{Re}\,\mathrm{e}^{in\tau} Z(i\tau)\mathrm{d}\tau = \frac{1}{2\pi}\int_{-\pi}^{\pi} \mathrm{Re}\exp\left[in\tau + \sum_{m=1}^{[\sqrt{n}]} \ln\left(1+\mathrm{e}^{-im^2\tau}\right)\right]\mathrm{d}\tau\,. \tag{6}$$

This integral formula is exact and may be used to compute $P(n)$ numerically for not too large n without much effort.

Figure 2 shows the function $g^{(1)}(E) = P(E)$ obtained from (6) replacing n by the continuous variable E; it may also be written as

$$g^{(1)}(E) = \sum_{m=0}^{\infty} P(m)\, j_0[\pi(E-m)]\,, \tag{7}$$

where $j_0(x) = \sin(x)/x$ is the spherical Bessel function of the order zero. As the figure shows, $g^{(1)}(E)$ is an analytical interpolation function yielding the exact values of $P(n)$ for integer $E = n$ (shown by the red crosses).

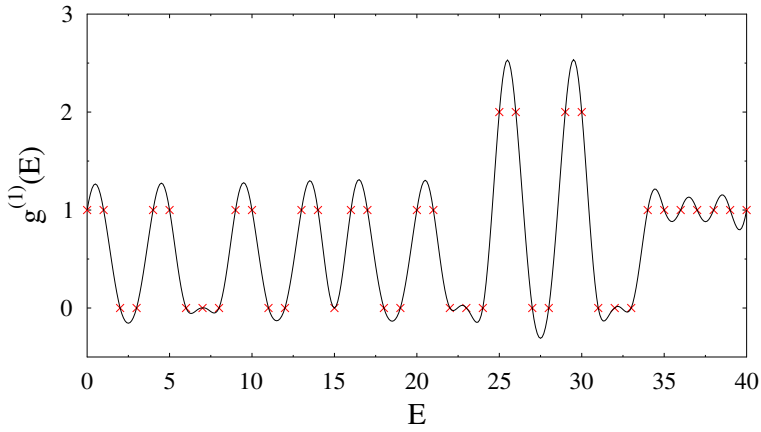

Fig. 2. (Colour on-line) The Bessel-smoothed partition density $g^{(1)}(E)$ (7) (black line) for small energies E. The red crosses at integer values $E = n$ show the exact values of $P(n)$.

2.2. Smooth part of $P(n)$

The smooth asymptotic part of a partition for large n can be obtained by quantum statistical methods (see also Ref. [10] for an article in number theory). In [4], the leading asymptotic smooth part of $P(n)$ was shown to be

$$P_{\rm as}^{(0)}(n) = \sqrt{\frac{\lambda_0}{6\pi}}\, n^{-5/6}\, \exp\left(3\lambda_0 n^{1/3}\right)\,, \tag{8}$$

with $\lambda_0 = 0.486227919$. Using the same quantum statistical method as in Refs. [5, 7], we derived in [6] an improved asymptotic expression

$$P_{\rm as}(n) = \sqrt{\frac{\lambda_0}{6\pi}}\, n^{-5/6}\, {\rm e}^{3\lambda_0 n^{1/3}} \left[1 - c_1\, n^{-1/3} - c_2\, n^{-2/3} - c_3\, n^{-1}\right]\,, \tag{9}$$

with $c_1 = 0.285645648$, $c_2 = 0.057115405$, and $c_3 = 0.020665371$. In Fig. 3, we show the leading approximation $P_{\rm as}^{(0)}(n)$ (8) (dashed line) and the improved result $P_{\rm as}(n)$ (9) (solid line). The latter is seen to give an excellent agreement with the average through the exact values of $P(n)$ (red crosses).

2.3. Fourier analysis of the partition density

In order to obtain a hint to the quantitative origin of the oscillations in $P(n)$, we study the Fourier transform (FT) of the partition density $g(E)$

$$\mathcal{F}_\tau[g(E)] = \int_{-\infty}^{+\infty} g(E)\, {\rm e}^{-iE\tau}\, {\rm d}E = F(\tau)\,. \tag{10}$$

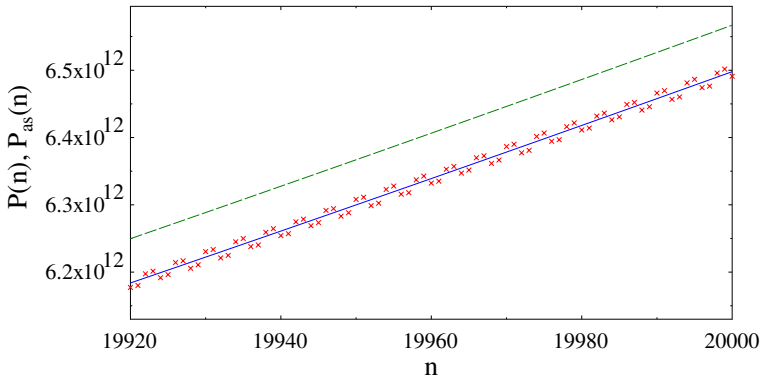

Fig. 3. (Colour on-line) Exact $P(n)$ by crosses (red), leading-order asymptotic part $P_{\rm as}^{(0)}(n)$ (8) by the dashed (green) line, and corrected asymptotic part $P_{\rm as}(n)$ (9) by the solid (blue) line in the large-n region.

Note that E and τ are a pair of conjugate dimensionless variables, such as energy and time. The absolute value of $F(\tau)$ can be written as

$$|F(\tau)| = \exp\left\{\mathrm{Re}\left[\ln Z(i\tau)\right]\right\} , \tag{11}$$

with $Z(\beta)$ given by the r.h.s. of Eq. (3). In the following, we show the amplitude $|F(\tau)|$ as a function of the frequency $f = 2\pi/\tau$ in units of the amplitude $I_0 = \exp(M \ln 2)$.

Figure 4 shows the Fourier spectrum as a function of $f = 2\pi/\tau$ for $2 \le f \le 22$ plotted on a logarithmical scale. The peaks are very sharp. We find peaks located exactly at $f = 3$, 4, 5, 9, 12, 13, 16, 20, and 21; all other peaks appear at rational frequencies. We can classify the peaks into *generations* with decreasing intensities. The vertical scale of Fig. 4 was selected such that the peaks of the generations 1–10 can be clearly differentiated; their (analytically calculated) scaled intensities are shown by the horizontal dashed lines.

When we first obtained this spectrum up to $f = 10$, we were struck by the two highest peaks at $f = 4$ and 5 (generations 2 and 1, respectively). Rajat, in his typical intuitive way, noted that these numbers appear in the smallest PT $(3, 4, 5)$. Before that time, we had not thought of Pythagorean triples at all. We extended the spectrum to higher frequencies and, indeed, found the peaks at $f = 13$ (generation 3, nearly degenerate with generations 4–7) and $f = 12$ (generation 8). These are members of the second-smallest PT $(5, 12, 13)$.

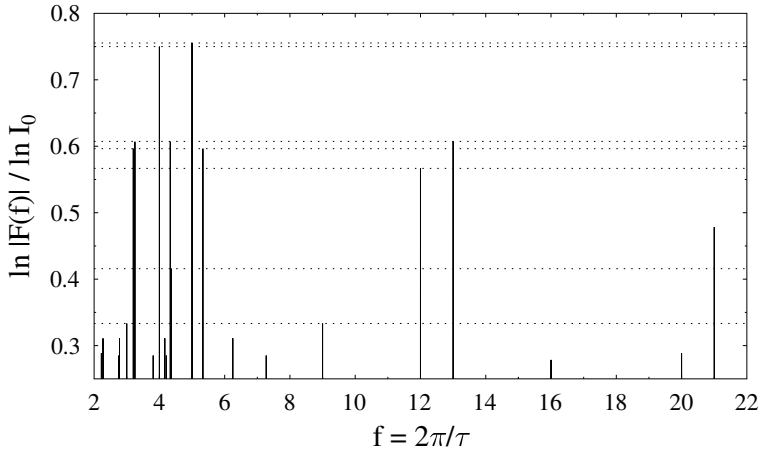

Fig. 4. Scaled Fourier transform $\ln|F(f)|$ of $g(E)$ on a logarithmic vertical scale. The horizontal dotted lines give the calculated relative intensities of the first 10 generations.

Figure 5 shows the same for f up to 105. Many more integer-valued frequencies appear. We notice, in particular, the dominating intensities of peak pairs with the frequencies of $(4, 5)$, $(12, 13)$, $(28, 29)$, $(36, 37)$, $(60, 61)$, $(84, 85)$, and $(100, 101)$. Four of them appear as the largest numbers in PTs, namely in $(3, 4, 5)$, $(5, 12, 13)$, $(11, 60, 61)$, and $(13, 84, 85)$. The numbers 28, 29 and 101 appear isolated in other PTs.

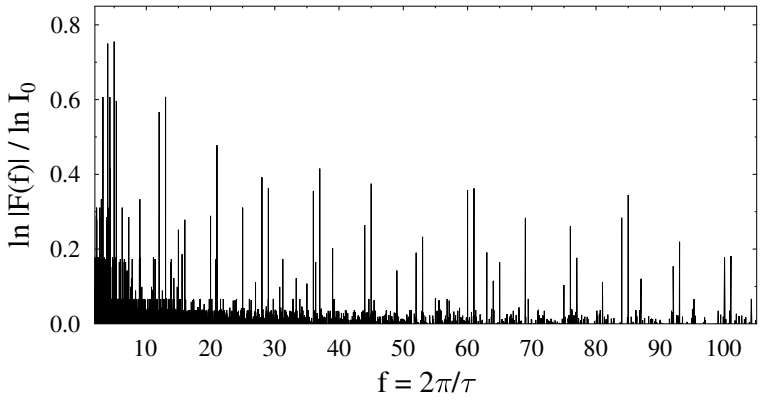

Fig. 5. The same as Fig. 4 over a larger range of the frequency f.

We had thus found a strong evidence that the PTs play a dominant role in the spectrum and hence also the oscillations of $P(n)$. This was confirmed quantitatively by the semiclassical trace formula presented next.

2.4. Trace formula for $\delta P(n)$

The main idea of our approach is the fact that asymptotic expressions of oscillating functions can be found from stationary-phase integration over saddles in the complex plane. Equation (6) of $P(n)$ can, in fact, be taken as an integral in the complex β plane, whereby the contour C goes along the imaginary (τ) axis from $-\pi$ to $+\pi$ yielding the exact $P(n)$. Since the integrand has no singularities for $x = \mathrm{Re}(\beta) > 0$, we may deform the contour arbitrarily, keeping its end points fixed. We choose it to pass over the most important saddles in the complex β plane corresponding to the leading Fourier peaks, and then use stationary-phase integration locally at each saddle. The smooth part $P_{\mathrm{as}}(n)$ is obtained from the real saddle point, while the summed contributions from the complex saddles yield an approximation for the oscillating part $\delta P(n)$.

Figure 6 shows a sketch of the situation in the complex β plane, with the deformed contour $\widetilde{C}$ chosen to pass over 5 representative saddles. The exact path between the saddles does not matter, since we only collect the local contributions near the saddles in the stationary-phase approximation. Each saddle can be associated to one of the Fourier peaks along the τ axis and hence to one of their frequencies f. The exact positions of the saddles in the β plane, and their properties needed for the stationary-phase integration (direction of the path of steepest descent and curvature at the saddle), could only be found numerically by scanning the landscape of the complex integrand of (6). In Ref. [6], we give analytical fits to the corresponding quantities and calculate the stationary-phase integrals.

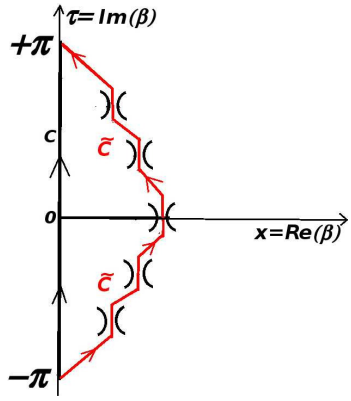

Fig. 6. (Colour on-line) Schematic plot of the contour integral (6). The exact contour C (from $-\pi$ to $+\pi$ along the τ axis) is deformed into a new contour $\widetilde{C}$ (grey/red) passing over selected saddles in the complex plane.

This yielded the following semiclassical trace formula for $\delta P(n)$:

$$\delta P(n) = \sum_{\tau_g > 0} A_g(n) \cos\left[n\,\tau_g - 3\mu_g\, n^{1/3} + \varphi_g\right], \qquad \tau_g \neq 2\pi k\,, \quad k \in \mathbb{N}_+\,, \tag{12}$$

where $\tau_g = 2\pi/f_g$ are the periods of the generations $g = 1, 2, \ldots$, and the amplitudes $A_g(n)$ are given by

$$A_g(n) = \frac{2}{(4\pi\kappa_g)^{1/2}}\, n^{-5/6}\, \mathrm{e}^{3\lambda_g\, n^{1/3}}\,. \tag{13}$$

The constants $\mu_g, \varphi_g, \kappa_g$, and λ_g are given in [6]. Note that $A_0(n)$ (*generation* 0) is identical with $P_{\mathrm{as}}^{(0)}(n)$ given in (8).

Figures 7 and 8 show the results of trace formula (12) by blue lines, compared to the exact $\delta P(n) = P(n) - P_{\mathrm{as}}(n)$ (red stars) in four ranges of n. The agreement between the two curves is excellent in all regions of n, the semiclassical results reproducing perfectly both the rapid oscillations of the exact $\delta P(n)$ and their beating amplitude.

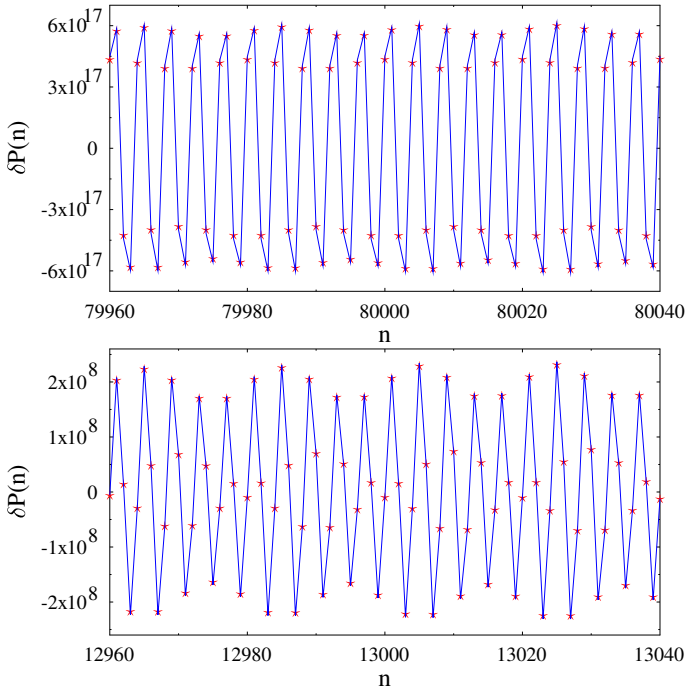

Fig. 7. (Colour on-line) Result of trace formula (12), shown by blue lines, *versus* the exact $\delta P(n) = P(n) - P_{\mathrm{as}}(n)$, shown by red stars, in two regions of large n.

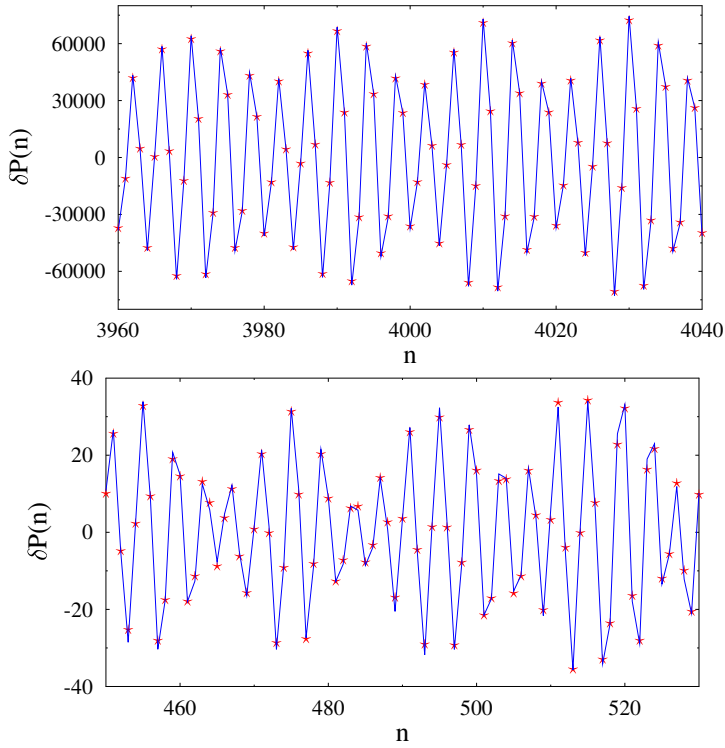

Fig. 8. The same as Fig. 7 in two regions of small n.

In the calculations for these results, the generations 1–10 have been included. However, nothing changes visibly in the results for $n \gtrsim 4\,000$ if we only include the two leading generations 1 and 2. While this might be a surprise at first sight, it can be explained by the values of the constants λ_g which regulate the exponential growth of the amplitudes $A_g(n)$. These are clearly higher for generations 1 and 2 than for the others.

The relative weights of the generations can be understood from Fig. 9, where we plot the amplitudes $A_g(n)$ on a logarithmic scale. The dash-dotted top line gives the amplitude of generation zero, which is identical with $P_{\rm as}^{(0)}(n)$. The solid (s) and dotted (d) lines give, from top to bottom, the amplitudes of the generations 2 (s), 1 (s), 6+7 (d), 3+4+5 (s), 8 (d), 10 (s), and 9 (d). Note that these amplitudes follow a slightly different ordering than those of the Fourier peaks in Figs. 4 and 5. The amplitudes of the generations 3 and higher are seen to be smaller than those of generations 1 and 2 by 2–3 orders of magnitudes for $n \gtrsim 5\,000$. These, in turn, are smaller than $P_{\rm as}(n)$ by 2–3 orders of magnitude, demonstrating the relative smallness of the oscillating part.

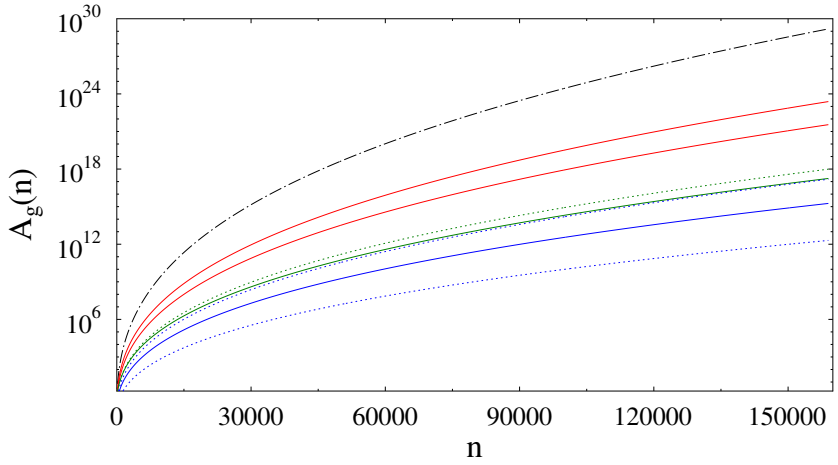

Fig. 9. Semiclassical amplitudes $A_g(n)$ for the generations (from top to bottom) 0 (giving the smooth part), 2, 1, $6+7$, $3+4+5$, 8, 10, 9 (see the text for details).

The relative importance of the higher generations for small n around ~ 80 can be studied in Fig. 10. Even here, the generations 1 and 2 produce the essential beating part of $\delta P(n)$. The inclusion of higher generations successively improves the semiclassical values of $\delta P(n)$, although their contributions are rather small and the convergence to the exact values is not as good as for $n \gtrsim 500$ (see Fig. 8). Together, these two figures demonstrate the overall rapid convergence of the trace formula upon summing over the generations g.

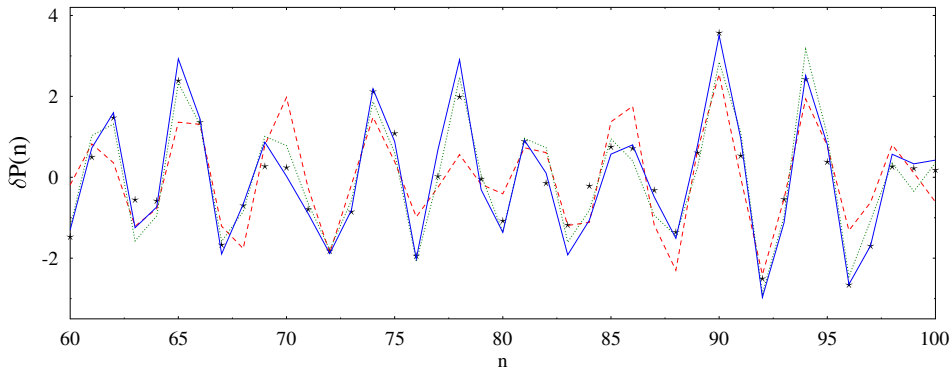

Fig. 10. (Colour on-line) Result of trace formula (12) around $n = 80$ for increasing numbers of generations included. Dashed line (red): generations 1 and 2; dotted line (green): generations 1–7; solid line (blue): generations 1–10. The stars (black) show the exact $\delta P(n)$.

We conclude that the oscillations in $\delta P(n)$ are dominated everywhere by the orbits of generations 1 and 2 with frequencies 4 and 5, which are members of the PT $(3,4,5)$. The contributions from all higher generations are practically negligible for $n \gtrsim 4\,000$ and still very small around $n \sim 500$. In order to understand the beat structure, one must realize that when studying $\delta P(n)$ as a function of n, the periods τ_g and frequencies $(2\pi/\tau_g)$ interchange their roles. The terms $\cos(n\tau_g + \ldots)$ in (12) have, as functions of n, the (approximate) periods $2\pi/\tau_g$ and hence frequencies τ_g. In the region where the beat structure is dominant, the period of the rapid oscillations is roughly that of the orbit with the largest amplitude (*i.e.*, τ_2 with frequency 4), while the beat comes from the difference in their frequencies: the period $\Delta n = 20$ of the beat is nothing but one over the inverse frequency difference $1/f_2 - 1/f_1 = 1/4 - 1/5 = 1/20$.

For $n \gtrsim 100\,000$, the beat structure fades away and the oscillations are practically given by the orbits of frequency 4 alone, as shown in Fig. 11 for n near 160 000. The exact values $\delta P(n)$, shown by the stars, exhibit no more beats. This is due to the fact that the amplitude of generation 2 here is nearly 2 orders of magnitude larger than that of generation 1.

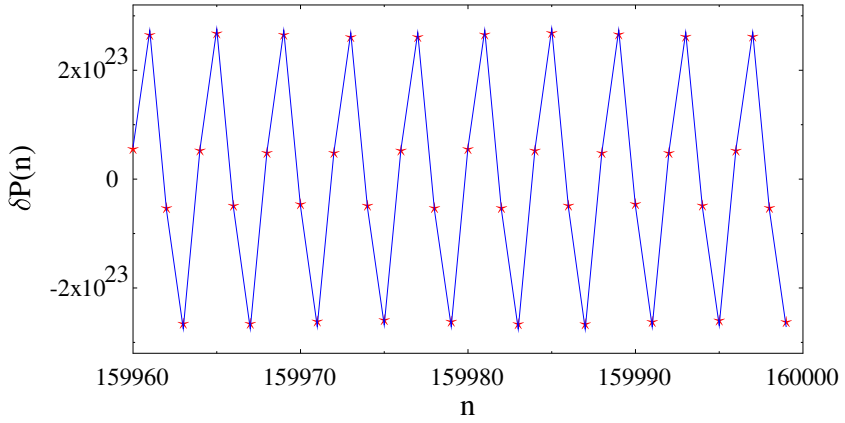

Fig. 11. (Colour on-line) Result of (12), shown by the blue line, using only the pair of orbits of generation 2 (with $f_2 = 4$), in the region near $n = 160\,000$. The exact $\delta P(n) = P(n) - P_{\rm as}(n)$ are shown by the red stars. Note that the beat structure in the exact $\delta P(n)$ has practically disappeared.

3. Summary

In summary, we have shown that a semiclassical trace formula, derived using the periodic orbit theory, is capable of reproducing the counting function $P(n)$ of the distinct square partitions not only qualitatively, but nearly

quantitatively, in particular in the asymptotic domain of large n. This demonstrates that semiclassical methods developed in physics can be successfully applied to number theory.

REFERENCES

[1] V.M. Strutinsky, *Yad. Fiz.* **3**, 614 (1966) [*Sov. J. Nucl. Phys.* **3**, 449 (1966)]; *Ark. Fys.* **36**, 629 (1966); *Nucl. Phys. A* **95**, 420 (1967); *ibid.* **122**, 1 (1968).

[2] M.C. Gutzwiller, *J. Math. Phys.* **12**, 343 (1971); R. Balian, C. Bloch, *Ann. Phys. (N.Y.)* **69**, 76 (1972); M.V. Berry, M. Tabor, *Proc. R. Soc. Lond. A* **349**, 101 (1976).

[3] M. Brack, R.K. Bhaduri, «Semiclassical Physics», *Bolder, Westview Press*, 2003.

[4] M.N. Tran, M.V.N. Murthy, R.K. Bhaduri, *Ann. Phys. (N.Y.)* **311**, 204 (2004).

[5] J. Bartel, R.K. Bhaduri, M. Brack, M.V.N. Murthy, *Phys. Rev. E* **95**, 052108 (2017).

[6] M.V.N. Murthy, M. Brack, R.K. Bhaduri, J. Bartel, *Phys. Rev. E* **98**, 052131 (2018).

[7] M.V.N. Murthy, M. Brack, R.K. Bhaduri, arXiv:1904.02776 [math.NT].

[8] «The On-Line Encyclopedia of Integer Sequences (OEIS)», http://oeis.org/

[9] D. Castelvecchi, *Nature* **531**, 287 (2016).

[10] R.C. Vaughan, *Ramanujan J.* **15**, 109 (2008).